ce/papers Proceedings in civil engineering

Ernst & Sohn A Wiley Brand

Check for updates

ORIGINAL ARTICLE

eurosteel AMSTERDAM 2023

Ernst & Sohn A Wiley Brand

I-beam to RHS-column joints with welded studs under cyclic loading

Ismael García[1] | Carlos López-Colina[1] | Miguel A. Serrano[1] | Yong Wang[2]

Correspondence

Dr. Ismael Garcia Garcia
University of Oviedo
Department of Construction and Manufacturing Engineering
Building 7, Campus Gijón,
33203
Email: garciaismael@uniovi.es

[1] University of Oviedo, Gijón, Spain
[2] The University of Manchester, Manchester M13 9PL, United Kingdom

Abstract

The design of removable beam-column joints between open structural steel beams and rectangular hollow section (RHS) columns is not easy because of the inaccessibility to the tube interior from outside. I-beam to RHS-column joints with threaded welded studs are of great interest due to their low-cost assembling technique and easy on-site execution. This study examines the cyclic performance of these joints with welded studs. A quasi-static experimental study on the cyclic response of eight joint specimens is described. The strength of the joint and the failure modes were revealed. The ductility of the joints was also evaluated according to the rotation capacity after yielding, classifying all of them as having intermediate ductility and, therefore, implying some capacity to withstand limited plastic deformations when subjected to seismic forces. Some equations were also used to classify the joints according to the components that mainly govern the deformation of the full joint. In addition, the energy dissipation rate was assessed for all the specimens, finding the highest energy dissipation rates in the most rigid joints.

Keywords

Tubular structures, Welded studs, Bolted connections, Joint characterization, Demountable joint, Cyclic behavior

1 Introduction

Steel structures are commonly used in a wide range of construction projects due to their excellent strength and durability. However, the design of removable beam-column joints connecting open structural steel beams to rectangular hollow section (RHS) columns is not easy because of the inaccessibility to the tube interior to tighten the bolts. The use of threaded welded studs for I-beam to RHS-column joints has garnered significant interest due to the convenience of the arc stud welding technique, which only requires access to one face of the workpiece to weld threaded studs. This feature makes it particularly suitable for the design and assembly of demountable joints with hollow sections due the fact the interior of hollow sections is typically inaccessible, rendering impossible the use of standard bolts.

Furthermore, the unavoidable static joint characterization, the performance of these structures under cyclic loading is a critical aspect that needs to be considered in the design and construction process, especially when the structures are under seismic actions. Standards for design of buildings and other civil engineering works such as Eurocode 3 part 1-8 [1], correctly describes partial-strength joints when subjected to static monotonic loading within the component method framework. However, when the joints are under cyclic loading, there is no direct and easy approach to characterize their cyclic behaviour and energy dissipation. This behaviour plays an important role in the global response of the structure which is affected by the ductility, rotation capacity, and energy dissipation of the joints [2].

The purpose of this study is to investigate the behaviour of beam-column connections with welded studs under cyclic loading and to determine their capacity for deformation, ductility, and energy dissipation. The study aimed to provide valuable information that can be used to improve the design and execution of joints with welded studs enhancing their safety and reliability.

To achieve this aim, the behaviour of beam-column joints with welded studs subjected to cyclic loads was studied by testing 8 beam-column joints with one-sided beam subjected to cyclic load. The ductility of the joints was also evaluated according to the rotation capacity after yielding. Some equations were also used to classify the joints according to their rotational capacity and attending the components that mainly govern the behaviour of the full joint. Finally, the energy dissipation rate was assessed for all the specimens.

https://doi.org/10.1002/cepa.2236 wileyonlinelibrary.com/journal/cepa

2 Experimental program

In order to study the behaviour of joints under cyclic loading, eight beam-column joints with one-sided beam were tested under cyclic loading, as shown in Figure 1. In the cyclic tests an upward/downward load was applied at the free end of the beam. As a result, it was necessary to anchor the column also at its upper part, fastening it to the reaction frame to prevent the specimen from moving upward when the actuator displacement was upward. The anchoring system to achieve this consisted of four threaded rods inserted through the hollow section of the column. These rods were threaded to nuts welded to the base plate arranged under the column and anchored by nuts and washers to a previously drilled steel plate placed at the top of the column, as shown in Figure 1.

(a)

(b)

Figure 1 Testing of joints under cyclic loading (a) and detail of anchoring system (b).

The geometry of the joints tested under cyclic loading are detailed in Table 1. The specimens were coded SCS1 to SCS9 (excluding SCS8, which was not prepared), referring to the same nomenclature used for monotonic specimens [3]. The beams spanned 840 mm in length, while the columns were 900 mm long. The tubes with a thickness of 6 mm were S275J0H while the columns with a thickness of 8 and 10 mm were made of steel S355J2H. The angle cleats were unequal L 120 × 80 × 10 made of S275JR steel. The studs used for these specimens were studs with a reduced diameter (RD studs) with metric of 20 mm and a steel grade of 4.8, as they showed a slightly more ductile behaviour than Grade K800 in monotonic tests [4]. The studs were prestressed to 150 Nm. The bolts used to connect the angle cleats to the beam flanges were Grade 10.9 instead of 8.8, which allowed the tightening torque applied to the bolts to be increased to 250 Nm and thus prevent slipping between the angle cleat and the beam flange.

Table 1 Geometries of the specimens tested under cyclic loads.

Joint	Column	Beam
SCS1	SHS 200×6	HEB 200
SCS2	SHS 200×8	HEB 200
SCS3	SHS 200×10	HEB 200
SCS4	SHS 200×6	IPE 300
SCS5	SHS 200×8	IPE 300
SCS6	SHS 200×10	IPE 300
SCS7	RHS 200×150×6	IPE 300
SCS9	RHS200×150×10	IPE 300

The cyclic load was applied to the free end section of the cantilever beam by clamping this section of the beam with a system of threaded rods and plates connected to a tie rod that couples to the actuator as shown in Figure 1 (a). A vertical displacement was applied upwards and downwards, following the quasi-static cyclic loading protocol proposed by FEMA 461 [5]. A total of thirteen displacement amplitudes were applied, with two cycles of the actuator up/down loading for each of the amplitudes. This protocol avoids an overestimation of the dissipating energy capacity of the joints [6]. Once the last amplitude was reached, the load was increased until failure occurred, which differs slightly from the original protocol due to execution time considerations. The selected amplitudes are included in Table 2 along with the displacement velocities used for each of the amplitudes, with the actuator displacement velocity increasing as the amplitude increases.

Figure 2 shows the moment-rotation curves of the specimens SCS5 and SCS6. The curves show a hysteresis behavior, where energy losses occur during cyclic loading and unloading. The energy dissipation is primarily attributed to the deformation of two components: angle cleats and front face. However, friction may play a secondary role in generating energy dissipation in the joints as friction can cause small energy losses during the relative movement of the parts. All specimens except for the SCS3, SCS6, and SCS9 joints eventually suffered a punching fracture of the stud on the front face of the tube. One example of this failure mode is shown in Figure 3. The SCS3 and SCS9 joints fractured due to the welded stud, while the SCS6 did not break due to an early termination

of the test by error. The resistant moments (M_R) and the maximum rotation of the joints under cyclic loads can be found in Table 3, while the stiffness of each joint under monotonic loads has been previously studied by the authors [7].

2.1 Deformation capacity of joints

The explicit classification of joints according to their rotational capacity is not included in the Eurocodes. Nevertheless, some authors [8] propose to classify joints according to their rotational capacity using a similar classification to that of section classification. The authors suggest classifying joints into three classes: class 1, class 2, and class 3. Thus, joints with unlimited deformation capacity that reach the design moment resistance with sufficiently good rotational capacity would be of class 1. Class 2 joints would be those capable of reaching the design moment but with limited deformation capacity. Joints of class 3 would be those where a failure due to brittleness or instability is what determines the resistant moment of the joint. This class of joints do not allow for complete internal force redistribution as they would have insufficient deformation capacity.

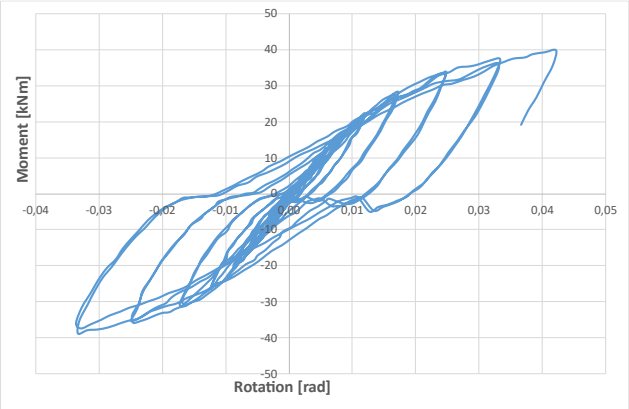

(a)

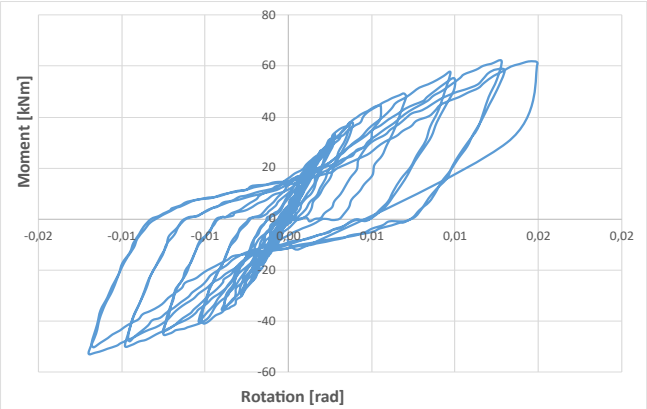

(b)

Figure 2 Moment rotation curves for specimen SCS5 (a) and SCS6 (b).

The deformation capacity of an angled bolted joint is governed by the predominant failure mode of the joint. Therefore, an early failure in components susceptible to brittle fracture (studs or bolts) should be avoided, so that the rest of the ductile behaviour components determine the behaviour of the joint. Thus, in this type of joint, failure must be governed by the strength of the angle cleats or the front face. When the joint has sufficient deformation capacity in at least one of these two components, it would have sufficient deformation capacity.

2.1.1 *Angle cleats-governed deformation capacity*

The deformation of an angle cleat joint with welded studs is governed by the deformation of the angle cleats, offering a high rotational capacity, assimilable to unlimited (plastic hinge) when the condition shown in equation (1) [9] is fulfilled, where t_l is the thickness of the angle cleats, d is the diameter of the studs, $f_{u,s}$ is the ultimate strength of the welded stud, and $f_{y,l}$ is the elastic limit of the angle cleats. Joints with reduced or limited plastic rotational capacity, but capable of reaching the design moment resistance without brittle fracture, would be those that meet the condition shown in equation (2). However, a plastic section verification is allowed. Joints that meet (3) would have insufficient deformation capacity.

$$t_l \leq 0.36 \cdot d \cdot \sqrt{\frac{f_{u,s}}{f_{y,l}}} \quad (1)$$ Unlimited deformation capacity

$$0.36 \cdot d \sqrt{\frac{f_{u,s}}{f_{y,l}}} < t_l < 0.53 \cdot d \cdot \sqrt{\frac{f_{u,s}}{f_{y,l}}} \quad (2)$$ Limited def. capacity

$$t_l \geq 0.53 \cdot d \cdot \sqrt{\frac{f_{u,s}}{f_{y,l}}} \quad (3)$$ Insufficient deformation capacity

Table 2 Displacement and velocity applied to the specimen in the test.

Δ [mm]	Velocity [mm/min]
1.1	1
1.6	1
2.3	2
3.2	2
4.4	3
6.2	3
8.6	4
12.1	4
16.9	6
23.7	6
30.8	8
37.9	8
45	8

2.1.2 *Front face-governed deformation capacity*

The deformation of a joint is mainly governed by the deformation of the front face and with a high deformation capacity, assimilable to unlimited when the condition

shown in equation (4) is met, where t_0 is the thickness of the column, d is the diameter of the stud, $f_{u,s}$ is the ultimate strength of the welded stud, and $f_{y,0}$ is the yield strength of the column. Joints with a reduced or limited plastic rotation capacity but able to reach the design moment without brittle fracture would be those that meet the condition shown in equation (5). In any case, a plastic verification of the section is allowed. Joints that meet (6) would have an insufficient deformation capacity.

$$t_0 \leq 0.36 \cdot d \cdot \sqrt{\frac{f_{u,s}}{f_{y,0}}} \quad (4)$$ Unlimited deformation capacity

$$0.36 \cdot d \cdot \sqrt{\frac{f_{u,s}}{f_{y,0}}} < t_0 < 0.53 \cdot d \cdot \sqrt{\frac{f_{u,s}}{f_{y,0}}} \quad (5)$$ Limited def. capacity

$$t_0 \geq 0.53 \cdot d \cdot \sqrt{\frac{f_{u,s}}{f_{y,0}}} \quad (6)$$ Insufficient deformation capacity

From equations (1) and (4), the maximum thickness of the angle and thickness of the front face of the column to have unlimited rotation is obtained. The results are shown in Table 4 for different column grades, metric and stud quality.

Figure 3 Failure mode of SCS5 specimen.

Table 3 Resistant moment (M_R) and rotation, Ductility (μ), total dissipated energy (E_T), dissipated energy at 1 rad (E_1), and energy dissipation ratio (R_{Ed}) of the cyclic specimens.

Joint	M_R [kNm]	Rot. [$mrad$]	μ	E_t [kJ]	E_1 [kJ]	R_{ED} [$\frac{kJ}{rad}$]
SCS1	29.9	44.5	2.2	5.9	3.4	5.8
SCS2	39.5	53.6	2.9	13.9	4.9	10.6
SCS3	41.8	59.7	2.6	15.0	5.1	9.2
SCS4	35.9	26.5	3.6	4.6	-	7.9
SCS5	41.4	42.2	2.9	6.3	5.4	9.7
SCS6	62.0	14.5	3.4	-	11.8	13.5
SCS7	36.0	38.7	3.6	7.7	-	11.4
SCS9	53.6	49.8	2.8	17.1	10.1	14.2

From the Table 4, it can be inferred that the specimens with columns with a thickness of 6 mm can be classified as joints with unlimited rotation capacity, with front face-governed deformation capacity. However, the specimens formed by columns with a thickness of 8 and 10 mm can be classified as joints with limited rotation capacity.

2.2 Ductility

Ductility is defined as the ability of a joint to plastically deform without a significant degradation in its strength [10]. The ductility ratio (μ) is used to assess the ductility of joints and can be calculated using equation (7), where Φ_y is the beam-column rotation at joint yielding, calculated from the skeleton curve (Figure 4), M_{max} is the maximum moment reached in the test, and Φ_{max} is the rotation at joint failure. To achieve this firstly, the skeleton curve, which is a graphical depiction that illustrates the response of a structural component or connection to varying levels of loading was calculated. Then, the moment and rotation at joint yielding calculated from the skeleton curve. Finally, the ductility ratio was obtained for the tested specimens. The results are shown in Table 3.

$$\mu = \frac{\Phi_{max}}{\Phi_y} \quad (7)$$

Table 4 Maximum thickness of the angle ($t_{l,max}$) and of the tube ($t_{0,max}$) to design joints with unlimited rotation capacity.

Column steel grade	RD Stud metric	Stud quality	$t_{l,max}$ [mm]	$t_{0,max}$ [mm]
S275	16	4.8	6	6
		K800	7	8
	20	4.8	7	8
		K800	9	10
S355	16	4.8	6	6
		K800	7	7
	20	4.8	7	7
		K800	9	9

2.3 Capacity for energy dissipation

The capacity for energy dissipation can be a measure of the deformation capacity of joints under cyclic loads [11]. From the tests, the energy dissipation in cyclic tests was evaluated. The area under the moment-rotation curve and the accumulated rotation was calculated for each joint. From that, the total dissipated energy (E_T) was calculated as the maximum energy reached, and the dissipated energy accumulated at 1 rad rotation (E_1). The rate of energy dissipation (R_{ED}) was calculated as the slope of the accumulated energy curve versus accumulated rotation and is also provided in Table 3. The apparently low energy dissipation exhibited by specimen SCS6 was due to an early stop of the test due to an error, after a loud noise during

the test that seemed to indicate failure. If the test had continued, it is expected the dissipated energy would have been higher.

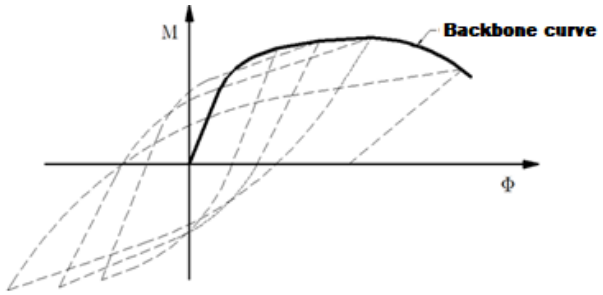

Figure 4 Example of backbone curve from moment-rotation curve in cyclic tests

Based on Table 3, the ductility of the joints ranged from μ= 2.2 to μ= 3.6. The analysis of the energy dissipation capacity of the joints showed that the specimens were able to dissipate energy ranging from 4.6 kJ (SCS4 specimen) to 17.1 kJ (SCS9 specimen), with an energy dissipation rate ranging from 5.8 kJ/rad (SCS1 specimen) to 14.2 kJ/rad (SCS9 specimen). It was also observed that specimens with higher rotational stiffness had a higher rate of energy dissipation.

3 Conclusions

The findings from the cyclic tests demonstrated that for a given specimen configurations (SCS1-SCS2-SCS3, SCS4-SCS5-SCS6, and SCS7-SCS9), the resistance moment of the joint increased as the tube thickness increased. Furthermore, it was observed that, by keeping the tube wall thickness constant (specimens SCS1-SCS4, SCS2-SCS3, and SCS3-SCS6), modifying the beam dimensions from an HEB 200 to an IPE 300 led to obtain a higher moment resistance. This indicates that a joint can withstand higher moments as the depth of the beam increases. These results are consistent with those obtained from monotonic tests.

The experimental tests revealed that the ultimate failure observed in the specimens formed with tube thicknesses of t_0=6 mm or t_0=8 mm, along with M20 studs, occurred due to punching shear of the studs into the front face of the tube. However, when the tube thickness was t_0=10 mm, the observed failure was due to fracture of studs. The specimens with columns with a thickness of 6 mm were classified as joints with unlimited rotation capacity, with front face-governed deformation capacity. However, the specimens formed by columns with a thickness of 8 and 10 mm were classified as joints with limited rotation capacity.

The ductility analysis of the specimens showed that all of them had a ductility value within the range of μ= 2.2 to μ= 3.6, suggesting that the specimens have some capacity for plastic deformation before failure. Therefore, following the classification proposed by Eurocode for sections [8], the joints could be classified as either class 1 or class 2. Furthermore, the rotation that occurred at the time of failure ranged from 26.5 mrad to 59.7 mrad, which, according to the provisions of 1998-1 [12], indicates that the joints can be considered of medium ductility class for use in seismic structures. According to ASISC 341-05 [13], the joints could be part of what the standard calls "intermediate moment frames" (IFM), indicating that it is expected that frames formed with this type of joint will withstand limited plastic deformation in their beams and joints when subjected to seismic forces. Finally, it was observed that specimens with higher rotational stiffness had a higher rate of energy dissipation.

References

[1] EN 1993-1-8:2005 - Eurocode 3: Design of Steel Structures - Part 1-8: Design of Joints. *Eurocode 3* 2005.

[2] Gioncu, V. Framed Structures. Ductility and Seismic Response. *J. Constr. Steel Res.* 2000, *55* (1–3), 125–154. https://doi.org/10.1016/S0143-974X(99)00081-4.

[3] Serrano-López, M. A.; López-Colina, C.; Wang, Y. C.; Lozano, M.; García, I.; Gayarre, F. L. An Experimental Study of I Beam-RHS Column Demountable Joints with Welded Studs. *J. Constr. Steel Res.* 2021, *182*, 106651. https://doi.org/10.1016/j.jcsr.2021.106651.

[4] García, I.; Serrano, M. A.; López-colina, C.; Gayarre, F. L.; Suárez, J. M. Approaches to the Mechanical Properties of Threaded Studs Welded to RHS Columns. *Materials (Basel).* 2021. https://doi.org/10.3390/ma14061429.

[5] Applied Technology Council. Interim Protocols For Determining Seismic Performance Characteristics of Structural and Nonstructural Components Through Laboratory Testing. *FEMA 461*. 2007.

[6] Bernuzzi, C.; Zandonini, R.; Zanon, P. Experimental Analysis and Modelling of Semi-Rigid Steel Joints under Cyclic Reversal Loading. *J. Constr. Steel Res.* 1996, *38* (2), 95–123. https://doi.org/10.1016/0143-974X(96)00013-2.

[7] García, I.; Serrano, M. A.; López-Colina, C.; Gayarre, F. L. The Stiffness of Beam-to-RHS Joints with Welded Studs. *J. Build. Eng.* 2023, *70*, 106340. https://doi.org/10.1016/j.jobe.2023.106340.

[8] Dujmovic, D.; Androic, B.; Piskovic, J. Modelling of Joint Behaviour in Steel Frames. In *Annual 2010/2011 of the Croatian Academy of Engineering*; Zagreb, 2012.

[9] Jaspart, J. P.; Weynand, K. Design of Hollow Section Joints Using the Component Method. In *Tubular Structures - Proceedings of the 15th International Symposium on Tubular Structures, ISTS 2015*; 2015. https://doi.org/10.1201/b18410-62.

[10] GB50011-2010. Code for Seismic Design of Buildings. 2010.

[11] Yin, Z.; Huang, Z.; Zhang, H.; Feng, D. Experimental Study on Energy Dissipation Performance and Failure Mode of Web-Connected Replaceable Energy Dissipation Link. *Appl. Sci. 2019, Vol. 9, Page 3200* 2019, *9* (15), 3200. https://doi.org/10.3390/APP9153200.

[12] Eurocode 8. Design of Structures for Earthquake Resistance—Part 1: General Rules, Seismic Actions and Rules for Buildings (EN 1998-1: 2004). *Eur. Comm. Norm. Brussels* 2004.

[13] ANSI/AISC. 360-16 Specification for Structural Steel Buildings. *Am. Inst. Steel Constr.* 2016.